ARMY RESEARCH LABORATORY

Energetics of Cation Radical Formation at the Proximal Active Site Tryptophan of Cytochrome-*c*-Peroxidase and Ascorbate Peroxidase

by G. M. Jensen, S. W. Bunte,
A. Warshel, and D. B. Goodin

ARL-TR-1859 December 1998

The findings in this report are not to be construed as an official Department of the Army position unless so designated by other authorized documents.

Citation of manufacturer's or trade names does not constitute an official endorsement or approval of the use thereof.

Destroy this report when it is no longer needed. Do not return it to the originator.

Army Research Laboratory
Aberdeen Proving Ground, MD 21005-5066

ARL-TR-1859 **December 1998**

Energetics of Cation Radical Formation at the Proximal Active Site Tryptophan of Cytochrome-*c*-Peroxidase and Ascorbate Peroxidase

G. M. Jensen, D. B. Goodin
Department of Molecular Biology, The Scripps Research Institute

S. W. Bunte
Weapons and Materials Research Directorate, ARL

A. Warshel
Department of Chemistry, University of Southern California

Abstract

Despite very similar protein structures, ascorbate peroxidase (APX) and yeast cytochrome-*c*-peroxidase (CCP) stabilize different radical species during enzyme turnover. Both enzymes contain similar active site residues, including the tryptophan that is oxidized to a stable cation radical in CCP. However, the analogous trytophan is not oxidized in APX, and the second oxidizing equivalent is retained as a porphyrin π-cation radical. In this study, we provide an improved computational approach to estimate the contribution of solvent and protein electrostatics to the energetics of tryptophan cation radical formation in the two enzyme environments. The Protein Dipoles Langevin Dipoles (PDLD) model is combined with molecular dynamics to estimate the role of discrete solvation, atomic polarizabilities, and dynamic motional averaging on the electrostatic potentials. The PDLD model shows that the protein environment of CCP stabilizes the tryptophan cation radical by 330 mV relative to that in APX. Analysis of the components contributing to this difference supports proposals that the cation binding site contributes to, but is not the sole cause of, the different sites of radical stabilization. The enzymes have thus evolved this distinction using several contributing interactions including the cation binding site, solvent access, and subtle differences in protein structure and dynamics.

Acknowledgments

The authors wish to thank Dr. C. S. Ashvar, Dr. Y. Cao, Dr. C. F. Chabalowski, Dr. M. M. Fitzgerald, Dr. D. Jollie, Dr. D. E. McRee, Dr. R. Musah, Professor P. J. Stephens, and S. K. Wilcox for helpful discussions, and Professor T. L. Poulos for helpful discussions and for providing the results of x-ray crystallography and other studies prior to publication. Research on Cytochrome-*c*-Peroxidase (CCP) at The Scripps Research Institute was supported by grants GM48495 and GM41049 (to Dr. Goodin) from the National Institutes of Health. The IBM 590 machines were made available by the Scripps Department of Molecular Biology. Mr. Bunte acknowledges financial support from the U.S. Army Research Laboratory (ARL) Director's Research Initiative Program. This work was also supported in part by a grant of high performance computing (HPC) time from the Department of Defense (DOD) HPC center, ARL, on the SGI Power Challenge Array.

INTENTIONALLY LEFT BLANK.

Table of Contents

INTENTIONALLY LEFT BLANK.

List of Figures

INTENTIONALLY LEFT BLANK.

List of Tables

INTENTIONALLY LEFT BLANK.

1. Introduction

Electron transfer occupies a position of central importance in biological systems. Understanding biological electron transfer requires an understanding of the proteins and enzymes with redox active cofactors precisely tuned to optimize (both thermodynamically and kinetically) their function [1]. The electrostatic environment of such a cofactor can extend significant control over its properties. If the cofactor incorporation into two proteins is similar (e.g., the same ligand set for a metal center), this control of redox functions by the protein should be amenable to computational modeling that includes cofactor, protein, and solvent elements.

The peroxidases comprise a class of enzymes that catalyze the H_2O_2 mediated oxidation of an enormous range of biological substrates [2, 3]. The heme containing enzyme cytochrome-*c*-peroxidase (CCP) from yeast reacts with H_2O_2 to form a two-electron oxidized intermediate: compound ES. This intermediate, in turn, accepts electrons sequentially from two ferrous cytochromes *c*. One oxidizing equivalent in compound ES is stored as an oxyferryl (Fe(IV)=0) heme, while the other is stored as a radical species on an amino acid side chain. In CCP, tryptophan-191 is preferentially oxidized to a π-cation radical to house the second oxidizing equivalent [4–9]. Tryptophan-191 in CCP is positioned as part of a so-called tryptophan-aspartate-histidine triad (the histidine being the heme ligand) thought to contribute to the stability of the indole cation radical on tryptophan-191 [10]. Ascorbate peroxidase (APX), a plant peroxidase that has a very similar molecular structure to CCP, including the tryptophan-aspartate-histidine triad, nevertheless does not exhibit an indole radical upon reaction with hydrogen peroxide [11–13]. Instead, a porphyrin π-cation radical is formed [14]. This difference in location of the stable second oxidation equivalent may be the cause of the different substrate preferences of the two peroxidases: large proteins for CCP (e.g., cytochrome *c*) and small molecules for APX (e.g., ascorbate). It is believed that in many other plant peroxidases, this is accomplished by replacing the triad tryptophan with another residue, such as phenylalanine, which is not so easily oxidized. In this report, we model the oxidation of tryptophan using the x-ray crystal structures of CCP and APX, atomic partial charges determined *ab initio,* and an

electrostatic/molecular dynamics program to model the protein and solvent. Calculations of the redox potential of the indole-to-indole cation radical oxidation in tryptophan-191 of CCP and in the analogous tryptohan-179 of APX reveal that the redox potential of the APX indole oxidation is ~330 mV higher than the equivalent reaction in CCP. This is sufficiently higher in APX to effectively account for the absence of an observed indole cation radical in APX. A bound monovalent cation observed in the APX structure ~9Å from the triad indole and absent in the CCP structure is partly, though not completely, responsible for the calculated increase in indole redox potential in APX relative to CCP, with other more structurally subtle factors comprising the remainder of the difference. These calculations build on earlier modeling studies [11–13], which used continuum models, which came to the same basic conclusions: There is an electrostatic origin of the destabilization of the triad tryptophan cation radical in APX relative to CCP, and this originates only in part from the K+ cofactor of APX.

2. Methods

The x-ray structure coordinates of pea cytosolic APX were kindly provided by Professor Thomas L. Poulos [11, 12, 13]; PDB accession number 1APX. The asymmetric unit of the crystal contains four identical monomers, which are labeled A, B, C, and D and which comprise two homodimers. These were utilized separately in the calculations. The crystal structure of recombinant yeast CCP was that of Goodin and McRee [10]; PDB accession number 1CCA; cf. Finzel, Poulos, and Kraut [15]. The crystal structure of M2301 CCP (from a different recombinant presentation) was that of Liu et al. [16]; PDB accession number 2CEP.

Electrostatic calculations of indole oxidation were performed using the program POLARIS and the Protein Dipoles Langevin Dipoles (PDLD) method [17–20]. The PDLD method has been applied to study the redox properties of heme in cytochrome *c* [21–23], of photosynthetic reaction centers [24], and of iron-sulfur proteins [25–28]. In each of these cases, some type of electrostatic representation (partial charges) for the cofactors within the proteins were derived from either *ab initio* or semiempirical methods.

The PDLD calculations were carried out using an IBM RS6000 implementation of the program POLARIS [18]. The redox active prosthetic group was defined to be region I and was in this case derived from a 3-methylindole moiety. The protein was truncated by a sphere of radius r_2 about the centroid of region I; the nonregion I protein atoms within this radius define region II. In the PDLD method, solvent water was modeled microscopically by a grid of orientable but positionally fixed Langevin dipoles. The Langevin dipole grid, region III, was generated within a sphere of radius r_L centered again about the region I centroid. In all cases, $r_L \geq r_2$. The Langevin system (region III) was further radially divided into an inner and outer region, the radius of the inner region being 12Å. The Langevin dipole grid spacing was 1Å and 3Å in the inner and outer portions of region III, respectively. Solvent water beyond region III was modeled macroscopically as a continuum dielectric (region IV) using a Born expression and a dielectric constant of 80.

Starting with the x-ray-derived structures, the crystallographically identified atoms assigned as water, O atoms were deleted. Hydrogen atoms are added using standard bond lengths and angles [18]. Where choices of H-atom placement were not obvious (e.g., a side chain OH group or histidine imidazole), the effects of varying these orientations on the calculations were examined and minimum energy positions were chosen. For protein atoms, heme, and K+, standard atomic partial charges, van der Waal's radii, and isotropic polarizabilities are used [18]. For the methylindole cofactor, partial charges for the oxidized and reduced states for region I atoms were derived by *ab initio* methods as discussed below. Langevin dipoles were deleted at grid points where the distance to any protein atom is less than the sum of the atomic van der Waal's radius and 1.4Å.

The PDLD model calculates the electrostatic contribution, ΔV, of the protein and solvent surrounding the redox active prosthetic group to the free energy difference of the oxidized and reduced states of the redox couple. ΔV is therefore a solvation energy for the reduction. ΔV is the sum of four terms, $\Delta VQ\mu$, $\Delta VQ\alpha$, ΔVL, and ΔVB, which are, respectively, the interaction of the region I atoms with the fixed partial charges of the protein atoms, the induced dipoles of the protein atoms arising from atomic polarizabilities, the Langevin dipole grid, and the continuum dielectric. $\Delta VQ\alpha$ was produced following self-consistent iteration in the field determined by protein atoms. Solvent water was modeled by orientable dipoles on a grid defined by a Langevin-Debye-type

equation. Orientation of the grid dipoles is carried out iteratively and is defined by the electric field resulting from protein partial charges, cofactor charges, and induced protein dipoles. ΔVL is the energy of interaction of the cofactor with the field defined by the solvent dipoles. All calculations unless otherwise specified use r_2 = 22Å and r_L = 25Å.

All calculations have been checked for convergence with respect to averaging over multiple Langevin grid positions, and iteration to achieve the self-consistent protein polarization field and Langevin dipole orientations. For CCP, arginine-48 is given a total charge of +1 and aspartate-235 is given a total charge of −1. For APX, the analogous arginine-38/aspartate-207 are given total charges of +1 and −1, respectively, and the K+ atom and liganding aspartate 187 are given total charges of +1 and −1, respectively. All other residues, the heme, and charged moieties at the surface of the proteins (heme propionates, residues such as aspartate, glutamate, arginine, and lysine) are modeled as neutral [26].

The free energy, ΔG, for the oxidation of a redox cofactor is the sum of the intrinsic energy of oxidation of that group and the solvation energy. While the latter is approximated by the PDLD method, the former is not in this case calculated, and therefore only differences in redox potential due to differences in the solvation energy ($\Delta\Delta V$) are modeled. In the present case, given the similarity of the structural environment of the triad tryptophan in CCP and APX, $\Delta\Delta V$ is likely to result from the relatively subtle differences in the electrostatics of these environments. Redox potential changes can be calculated for tryptophan in APX and CCP by the PDLD method, these being obtained by using $\Delta\Delta V$ for the two proteins and the conversion factor 23.06 cal/mV. Molecular dynamics (MD) were also applied starting with the x-ray structures and using the program POLARIS [18, 26, 27, 28] in order to provide the proper averaging over configurations generated in both redox states. Doing so provides the effect of protein reorganization and yields the proper free energy within the linear response approximation [18, 19]. MD is limited to atoms lying within a sphere of radius 12Å, centered at the region I centroid. In addition, during MD, Cartesian constraints are applied in APX to the K+ and aspartate-187 Oδ atoms, and in both CCP and APX at the aspartate-235/207 Oδ, the heme liganding histidine-175/163 Nε, and tryptophan-191/179 Nε atoms. These constraints take the form of isotropic atomic harmonic potentials whose minima are at the

crystallographic atomic positions and whose force constants (k) are 50 kcal/Å^2 for the K+/ligating Oε and 150 kcal/Å^2 for the tryptophan Nε aspartate Oδ and histidine Nε pairs. MD was run for 25 ps at 300 K. PDLD calculations were carried out on 50 MD structures taken at 0.5-ps intervals. The results were averaged together with a t = 0 value to yield MD-averaged values of ΔV.

We have previously reported results of *ab initio* calculations of gas-phase structures, energies, harmonic vibrational frequencies, infrared and Raman intensities, and atomic spin densities of 3-methylindole (skatole), 3-methylindole neutral radical, and 3-methylindole cation radical [9, 29]. These calculations employed density functional theory, the Becke3LYP functional [30, 31] as implemented in Gaussian 92/DFT or Gaussian 94 [32], and the 6-31G* and TZ2P basis sets [33]. This level of theory has been shown to be capable of providing accurate predictions of properties for open shell molecules [34, 35]. From the 6-31G* calculations, the atomic partial charges used for this study were determined using the electrostatic potential (ESP) methods developed by Kollman and coworkers [36, 37]. Specifically, fitted ESP charges were obtained with the Merz-Kollman option in Gaussian 94. This method places points at which the ESP is evaluated on four shells around each atom an increasing distance from each nucleus (1.2-, 1.4-, 1.8-, and 2.0-times the van der Waal's radius of that nucleus). The points are placed at a uniform spacing of 1 pt/Bohr on each surface. The atomic-centered charges are fitted to the values of ESP with a Lagrange undetermined multiplier matrix solution that permits constraints to be applied to the system. The only constraint used here was that the sum of the atomic charges equals the molecular charge. Since this process determines the atomic partial charges, which give a best fit to the ESP on a surface surrounding the molecule, they are expected to be useful when imported into protein electrostatic models, such as is implemented in the PDLD method. In order to assess the effects that the polar protein environment might have on the *ab initio* properties of the indole, further calculations at the Beck3LYP 6-31G* geometry were carried out with point charges placed to correspond to the CO_2 moiety of aspartate-235 of CCP (−0.75 for each oxygen, +0.5 for the carbon) and for the amide groups of amino acids 175 and 177 of CCP (±0.5 for the C=O moiety, ±0.45 for the NH moiety). These point charge positions were determined by fitting the 3-methylindole molecule onto tryptophan-191 of CCP using the program Xtalview [38] and outputting the coordinates of the 3-methylindole, CO_2, and NHCO moieties for input into Gaussian. The calculation of the atomic

charges in the presence of the background charge distribution was done using the Gaussian implementation of the method of Hall and Smith [39, 40].

3. Results and Discussion

Figure 1 shows views of the heme active site and tryptophan-aspartate-histidine triad containing regions of the structures of CCP and APX. Clearly, the structures are very similar to one another in this region, despite having very different substrate specificity. The similarity of structure is much less surprising in view of the ~33% sequence identity between the two peroxidases [41]. Also shown in Figure 1 are positions of Langevin dipole grid points, illustrating the similar degree of solvent penetration into this region of the protein for both enzymes. Figure 2 shows the structure and atom numbering for the analog 3-methylindole cation radical used to model the tryptophan. Also shown are the ESP-derived partial charges for the cation radical at the Becke3LYP/6-31G* level of theory. Table 1 shows partial charges for 3-methylindole and for the cation radical and the values translated onto the triad tryptophan species in CCP and APX (tryptophan-191 and tryptophan-179, respectively) for use in the electrostatic calculations. Clearly, the cationic character of this radical is distributed over the whole indole moiety. The benzene and pyrrole moieties, for example, have total charges of 0.44 and 0.65, respectively, and the relative charge distribution is not altogether different from unoxidized 3-methylindole. Therefore, the analysis of electrostatic stabilization by either the nearby triad aspartate in CCP and APX or the more distant K+ cation in APX is more complex than a simple Coulombic interaction between two point charges. In APX (structure A), the distances between the K+ cation and the tryptophan side chain atoms range from 8.7Å (Cγ) to 11.5Å (Cζ2). Complicating this analysis is the fact that the K+ cation is more properly viewed as an aspartate-187-K+ dipole, with an overall neutral charge (aspartate-187 is the only charged ligand to the K+ binding site). This dipole will have a less straightforward and steeper distance dependence in terms of interaction with a cation radical at the triad tryptophan.

Table 2 shows results of POLARIS calculations for CCP and for structures A, B, C, and D of APX. Overall, ΔV for CCP is larger than ΔV for any of the APX structures. (Under the sign

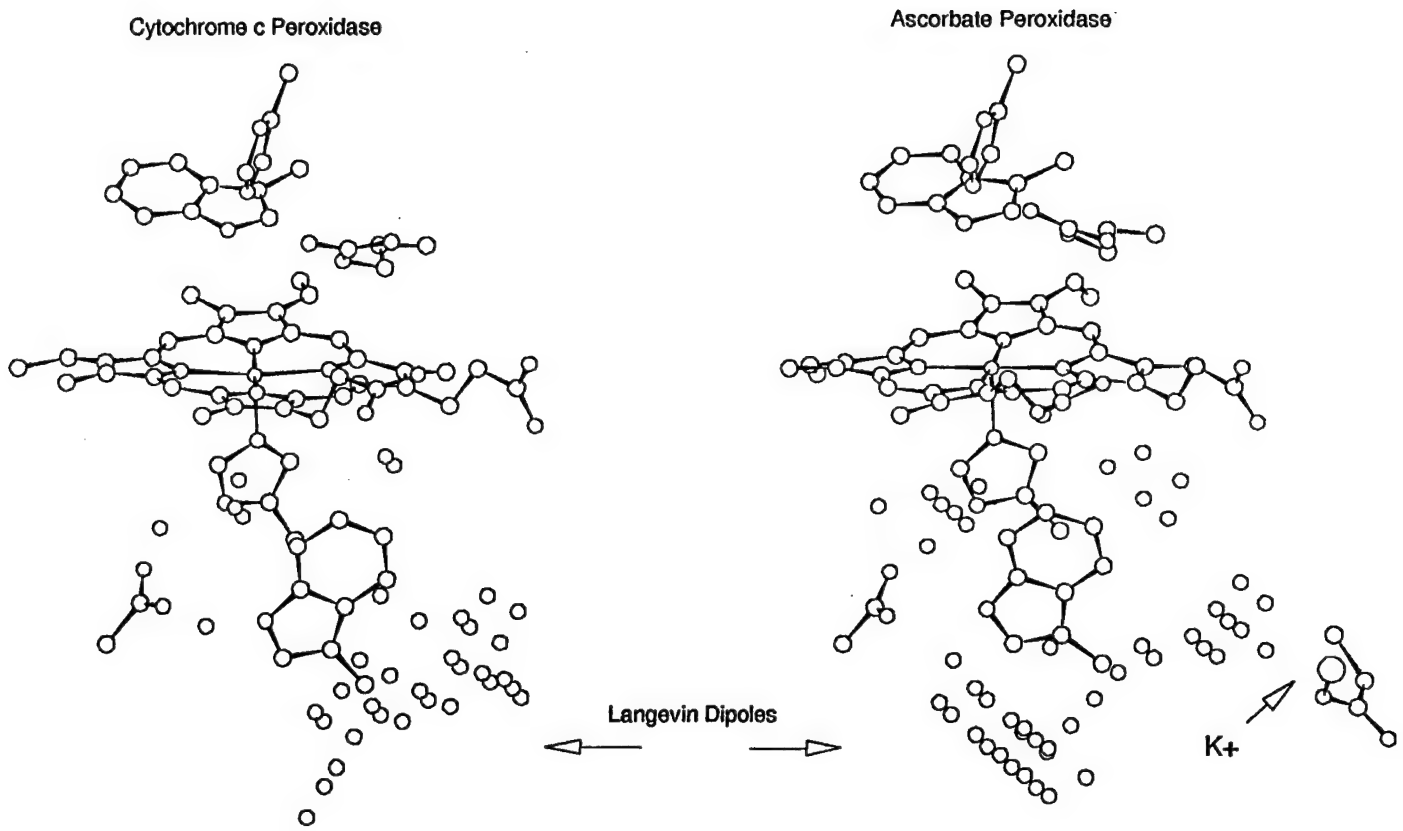

Figure 1. The Active Sites of Cytochrome-*c*-Peroxidase (CCP) and Ascorbate Peroxidase (APX); Structure A. Depicted for Both Proteins Are the Distal Histine, Tryptophan and Arginine, the Heme, and the Triad of Tryptophan, Aspartate, and Histidine. Shown for APX Is Also the Aspartate-Potassium Binding Site. For Both Proteins, the Locations of Langevin Dipoles From One of the Dipole Grids Utilized in PDLD Calculations Are Represented as Small Spheres (See Section 2, Methods).

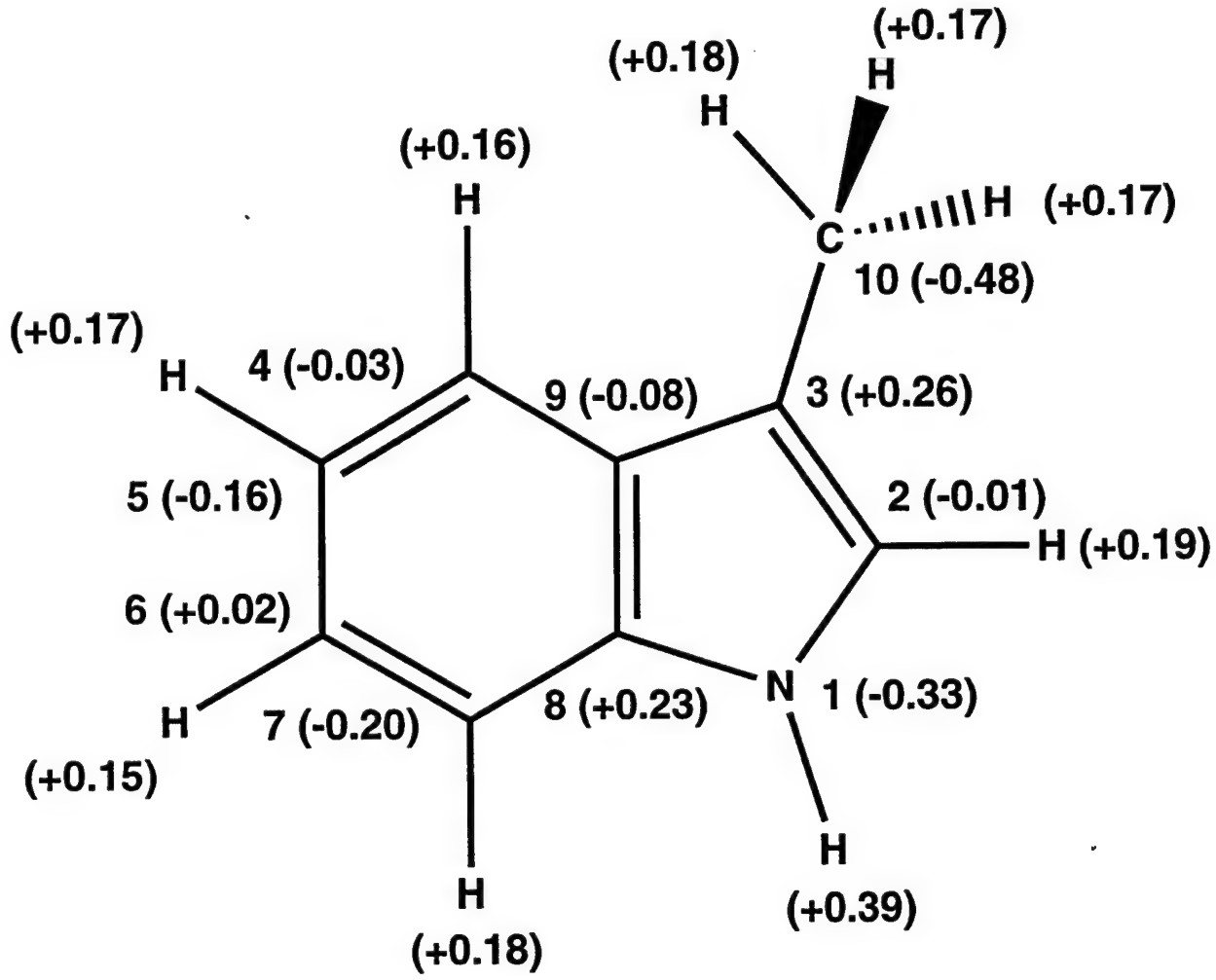

Figure 2. Atom Numbering and Becke3LYP/6-31G* ESP Charges (in Parentheses) for 3-Methylindole Cation Radical.

radical state relative to the unoxidized state.) The range of ΔΔV values (ΔV for APX - ΔV for CCP) is −3.5 to −7.8 kcal/mole for the four available APX substructures. This translates to an average redox potential difference of −279 mV (range −150 to −339 mV). The primary origin of this difference is in the first Polaris term, ΔVQμ, which is between 16–20 kcal/mole larger in CCP than APX. The protein polarization term, ΔVQα, is small and positive in APX, and for CCP, it is −6.6 kcal/mole. The value ΔVL also contributes significantly to ΔV for each structure, and overall, the sum of ΔVQα and ΔVL serves to dampen some of the initial difference seen in ΔVQμ. ΔVB

Table 1. Partial Charges[a]

Atom Numbering (Tryptophan)	Atom Numbering (3-Methylindole)	ESP Charges		Charges Used in PDLD Model		External Charges
		3-Methylindole	3-Methylindole Cation Radical	Tryptophan	Tryptophan Cation Radical	3-Methylindole Cation Radical
Nε1	1	−0.42	−0.33	−0.42	−0.33	−0.35
Cδ1	2	−0.20	−0.01	−0.20	−0.01	0.00
Cγ	3	0.08	0.26	0.08	0.26	0.23
Cε3	4	−0.18	−0.03	−0.18	−0.03	−0.01
Cζ3	5	−0.17	−0.16	−0.17	−0.16	−0.18
Cη2	6	−0.10	0.02	−0.10	0.02	0.03
Cζ2	7	−0.26	−0.20	−0.26	−0.20	−0.21
Cε2	8	0.21	0.23	0.21	0.23	0.25
Cδ2	9	0.02	−0.08	0.02	−0.08	−0.07
Cβ	10	−0.36	−0.48	−0.36	−0.48	−0.48
Hε1	—	0.36	0.39	0.36	0.39	0.40
Hδ1	—	0.18	0.19	0.18	0.19	0.20
Hε3	—	0.14	0.16	0.14	0.16	0.15

[a] Partial charges are determined as described in the Methods section. Atom numbering for 3-methylindole is as described in Figure 2. The "External Charges" set are ESP charges resulting from inclusion of external charges in the *ab initio* calculation as described in the Methods section.

Table 1. Partial Charges (continued)[a]

Atom Numbering (Tryptophan)	Atom Numbering (3-Methylindole)	ESP Charges		Charges Used in PDLD Model		External Charges
		3-Methylindole	3-Methylindole Cation Radical	Tryptophan	Tryptophan Cation Radical	3-Methylindole Cation Radical
Hζ3	—	0.12	0.17	0.12	0.17	0.17
Hη2	—	0.12	0.15	0.12	0.15	0.15
Hζ2	—	0.14	0.18	0.14	0.18	0.18
Hβ1, Hβ2	(skatole methyl)	0.10, 0.10, 0.10	0.17, 0.17, 0.18	0.16, 0.16	0.27, 0.27	0.17, 0.17, 0.18
Cα	(backbone)	—	—	-0.097	-0.097	—
Hα	(backbone)	—	—	0.097	0.097	—
HN	(amide)	—	—	0.45	0.45	—
N	(amide)	—	—	-0.45	-0.45	—
C	(amide)	—	—	0.50	0.50	—
O	(amide)	—	—	-0.50	-0.50	—

[a] Partial charges are determined as described in the Methods section. Atom numbering for 3-methylindole is as described in Figure 2. The "External Charges" set are ESP charges resulting from inclusion of external charges in the *ab initio* calculation as described in the Methods section.

Table 2. PDLD Results With X-ray-Derived Structures[a]

Protein	ΔVQμ (kcal/mol)	ΔVQμ (kcal/mol)	ΔVL (kcal/mol)	ΔVB (kcal/mol)	ΔV Total (kcal/mol)	ΔΔV (kcal/mol)	ΔΔV(mV)	Average ΔΔV (mV)
MKT	53.67	−6.57	2.92	5.49	55.51	0.00	0	0
APXA	33.27	2.82	4.47	7.71	48.27	−7.24	−314.0	−278.9
APXB	37.32	0.86	5.39	8.48	52.05	−3.46	−150.0	—
APXC	37.95	0.92	3.94	4.89	47.70	−7.81	−338.7	—
APXD	33.47	2.52	5.53	6.77	48.29	−7.22	−313.1	—
APXANOK	41.63	−2.88	−0.05	7.21	45.91	−9.60	−416.3	−260.3
APXBNOK	43.98	−3.15	3.94	8.40	53.17	−2.34	−101.5	—
APXCNOK	44.92	−3.43	2.97	5.00	49.46	−6.05	−262.4	—
APXDNOK	38.19	−0.65	5.09	6.86	49.49	−6.02	−261.1	—
M2301	46.11	−4.03	3.92	6.38	52.38	−3.13	−135.7	−135.7

[a] MKT is the crystal structure of CCP; APX A, B, C, and D are the four x-ray coordinate sets from the crystal structure of APX; the "NOK" suffix results from calculations where the aspartate-187/K+ charges are set individually to zero; and M2301 is the x-ray structure of CCP with methionine mutated to isoleucine. Other details of the x-ray structures used and calculational methods employed are provided in the Methods section. Average refers to averaging results for APX structures A through D. ΔΔV is calculated relative to CCP.

is relatively invariable for each structure. Details of the origin of these terms in CCP and APX follow.

An important observation of this study is the variation in the electrostatic energies for the four examples of the APX structure within the crystal asymmetric unit (the overall root mean square positional deviation for Cα atoms is ≤0.4Å for any given pairwise comparison of the four structures) [11–13]. Differences in these four structures most likely result from packing effects and may reflect average snapshots of the range of conformers available to the protein in solution. In other studies using the PDLD method to study redox potentials, great benefit in terms of method accuracy was realized from generating a family of structures by MD from any x-ray derived structure [18, 19, 20, 26, 27, 28]. The improvement might in any given case result from adjusting structural elements that are not energetically reasonable, sampling a range of thermally accessible structures rather than the x-ray-derived average, improving the convergence of the iterative aspects of the PDLD model (especially in the solvent mode), sampling multiple orientations for the placement of freely orientable hydrogens, inclusion of protein reorganization energy, or all of the above. Figure 3 shows ΔV determinations for 51 structures generated during MD for CCP and APX (structure A, t=0 and 25 ps of dynamics with 0.5-ps snapshots; structures B, C, and D had similar profiles). Figure 4 shows the structures of the snapshot samples for CCP. MD averaged values for all of the structures are shown in Table 3. In each case, ΔV for a given structure decreased upon MD averaging. In addition, the spread in ΔV values for the four APX structures decreases, and $\Delta\Delta V$ for the average of all four APX structures vs. CCP decreases to −7.6 kcal/mole or −330 mV.

The fully averaged (MD, multiple structures) values of $\Delta\Delta V$ provide for the prediction that tryptophan-179 in APX is 330 mV more difficult to oxidize to the radical cation than tryptophan-191 in CCP. Mondal, Fuller, and Armstrong [42] have reported that the midpoint potential of this oxidation in CCP is +740 mV vs. S.H.E. This places the estimated potential for APX at greater than 1 V, which is higher than the midpoint potential for indole water [43]. We cannot at this time rule out all other options for the absence of an observed tryptophan radical cation in APX. The radical could exist but have a lifetime too short to observe under the experimental conditions employed to date, the porphyrin π-cation radical that is observed could simply be unusually stable in APX relative

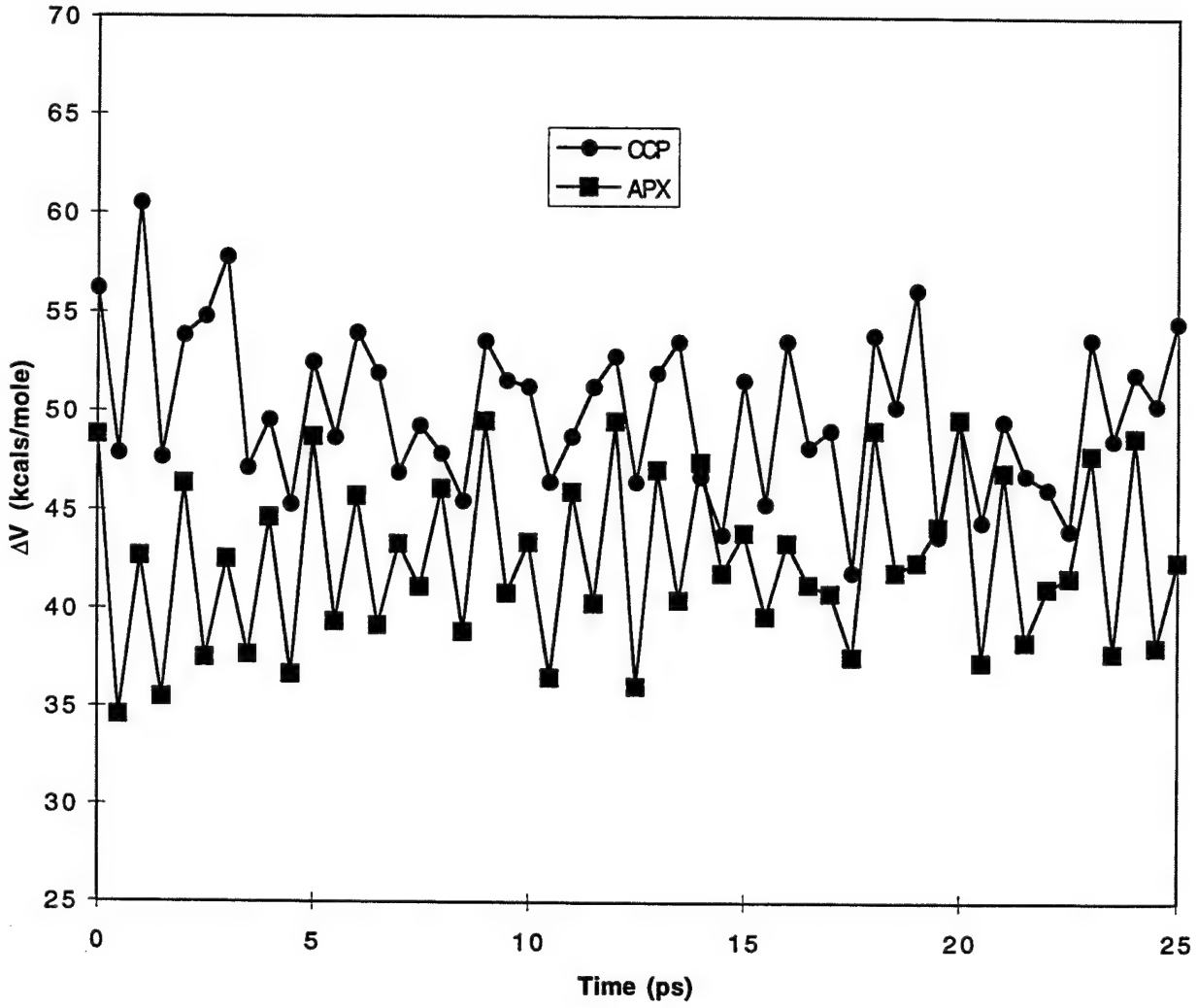

Figure 3. Values of ΔV for APX (Structure A) and CCP Over 25 ps of Molecular Dynamics.

to CCP, or there could be a kinetic barrier to oxidation of tryptophan in APX sufficient to divert the second oxidizing equivalent elsewhere. Also, the minimum value of the midpoint potential shift from CCP to APX sufficient to shunt the second oxidizing equivalent of H_2O_2 to another site is not known. However, these calculations do show that electrostatic differences alone between CCP and APX are large enough to explain the thermodynamic instability of this radical species in APX on reaction with H_2O_2. This conclusion is consistent with the observation that cation binding sites can be created in the active site of CCP by cavity-forming site-directed mutants [44–53]. Given a tryptophan site electrostatically predisposed for stabilizing a cation, it is also not surprising to note that the structure of CCP is little changed upon oxidation to compound ES [54].

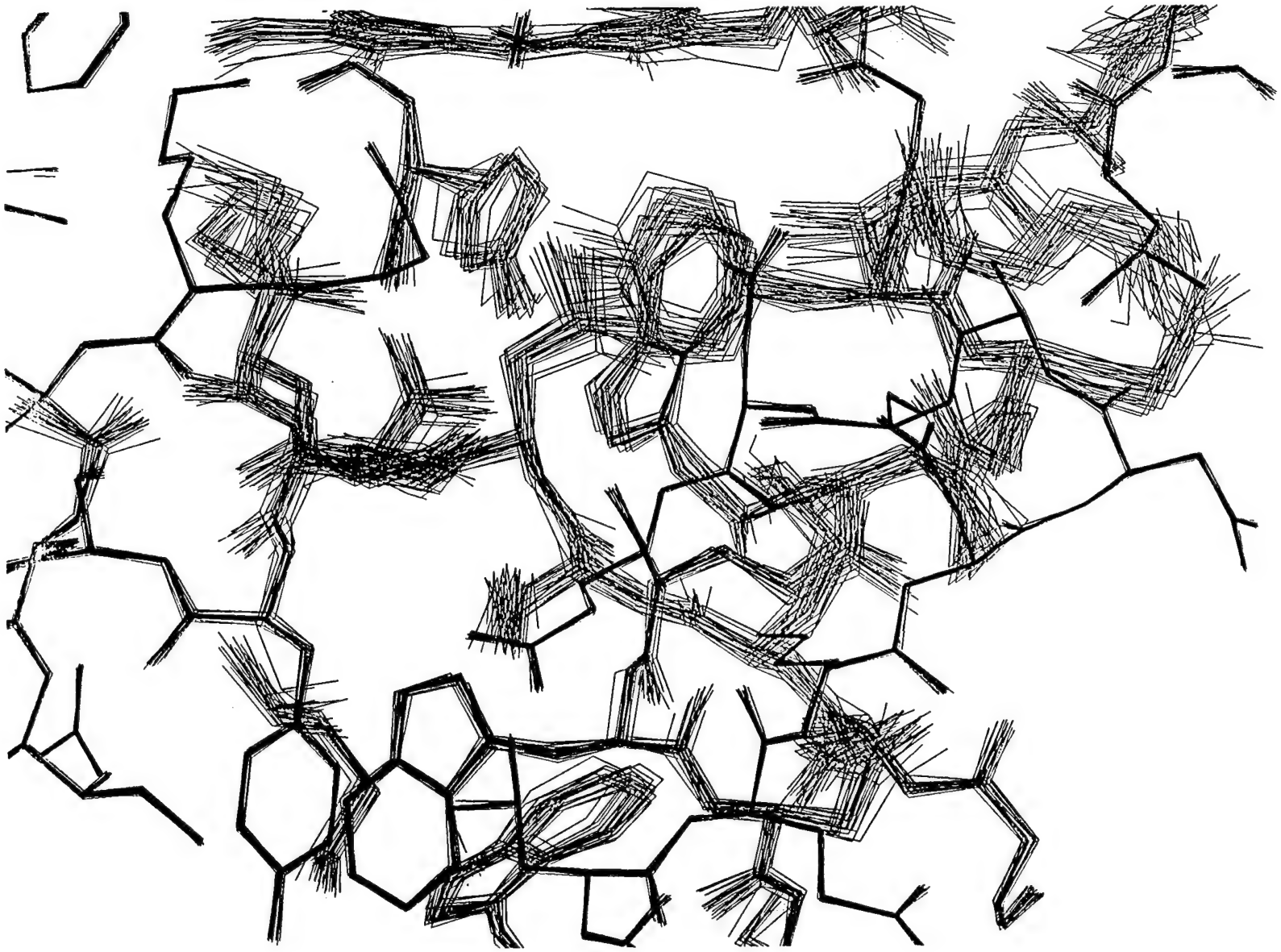

Figure 4. Fifty-One Superposed "Snapshot" Structures From a 25-ps Molecular Dynamics Run for CCP. PDLD Calculations for These Structures Are Utilized to Determine Structure-Averaged Results.

Table 3. PDLD Results From MD Averaging of X-ray Structures[a]

Protein	ΔV (kcal/mol)	ΔΔV (kcal/mol)	Average ΔV (kcal/mol)	Average ΔΔV (kcal/mol)	ΔΔV (mV)	Average ΔΔB (mV)
MKT	50.00	0.00	—	—	0	—
APXA	42.40	-7.60	42.43	-7.58	-329.6	-328.5
APXB	43.70	-6.30	—	—	-273.2	—
APXC	42.00	-8.00	—	—	-346.9	—
APXD	41.60	-8.40	—	—	-364.3	—
APXANOK	41.30	-8.70	42.90	-7.10	-377.3	-307.9
APXBNOK	45.20	-4.80	—	—	-208.2	—
APXCNOK	41.70	-8.30	—	—	-359.9	—
APXDNOK	43.40	-6.60	—	—	-286.2	—
M2301	50.30	0.30	0.30	0.30	13.0	—

[a] Coordinate sets are as defined in Table 2 and the Methods section. Details of the calculations are provided in the Methods section. All results are MD averages; "average" refers to averaging values for structures A through D. ΔΔV is calculated relative to CCP.

To trace the structural origin of the electrostatic differences seen in the calculations of $\Delta\Delta V$, we examined the individual protein residue contributions to $\Delta VQ\mu$, since this term dominates the difference in $\Delta\Delta V$. Figure 5 displays a profile of per residue contributions to $\Delta VQ\mu$ for both CCP and APX (structure A is shown; structures B, C, and D are all very similar). The homology between the two proteins is obvious. Prominent features (moving linearly in sequence space), which contribute about equally in CCP and APX, are from the distal arginine cation (48 in CCP, 38 in APX), the trio of backbone carbonyl groups from residues 172, 175, and 177 in CCP and 160, 163, and 165 in APX, and the active site aspartate (235 in CCP, 207 in APX). The three major differences between CCP and APX are the larger contribution of the 172/175/177 backbone carbonyl trio in CCP relative to the 160/163/165 trio in APX (18.7 vs. 13.2 kcal/mole), the significantly larger contribution attributed to methionine 230 in CCP relative to leucine 203 in APX, and the presence in APX of the aspartate 187/K+ dipole with no equivalent in CCP. Table 4 lists the values $\Delta VQ\mu i$ for each of these interactions as well as other smaller contributions.

All the significant contributions noted here are within 15Å of the triad tryptophan. Calculations run with r_2 set at (r_L = 25Å) give $\Delta\Delta V$ values essentially identical to those reported with r_2 = 22Å (data not shown), confirming the relatively local nature of the origin of $\Delta\Delta V$. The distal arginine (48 in CCP, 38 in APX) resides in a partially solvent-filled cavity on the distal side of the heme with a nearest approach of ~7Å to the relevant tryptophan. Calculations with this residue modeled as electroneutral yield $\Delta\Delta V$ values essentially identical to those which use a charge of +1 on this residue (data not shown). Methionine 230 contributes to $\Delta VQ\mu$ from both the polar side chain (S_δ is ~5Å from tryptophan 191) and from the backbone carbonyl (which oxygen is ~3Å from the tryptophan). Leucine 203 in APX has a nonpolar side chain and, in addition, has a less favorable orientation of the corresponding backbone carbonyl relative to CCP. We have performed calculations using the structure for the CCP mutant where methionine 230 is replaced by isoleucine (M230I) [16]. Results for the x-ray structure and for MD average structures are presented in Tables 2 and 3. Using the x-ray structure, there is a 8 kcal/mole decrease in $\Delta VQ\mu$ in M230I-CCP relative to CCP, which contributes to a $\Delta\Delta V$ of -3.1 kcal/mole or -136 mV. MD averaging for this structure, however, reduces $\Delta\Delta V$, now positive, to only 0.3 kcal/mole or 13 mV. Experimentally, although the kinetics for reaction of H_2O_2 were altered by the M230I mutation [16], a tryptophan

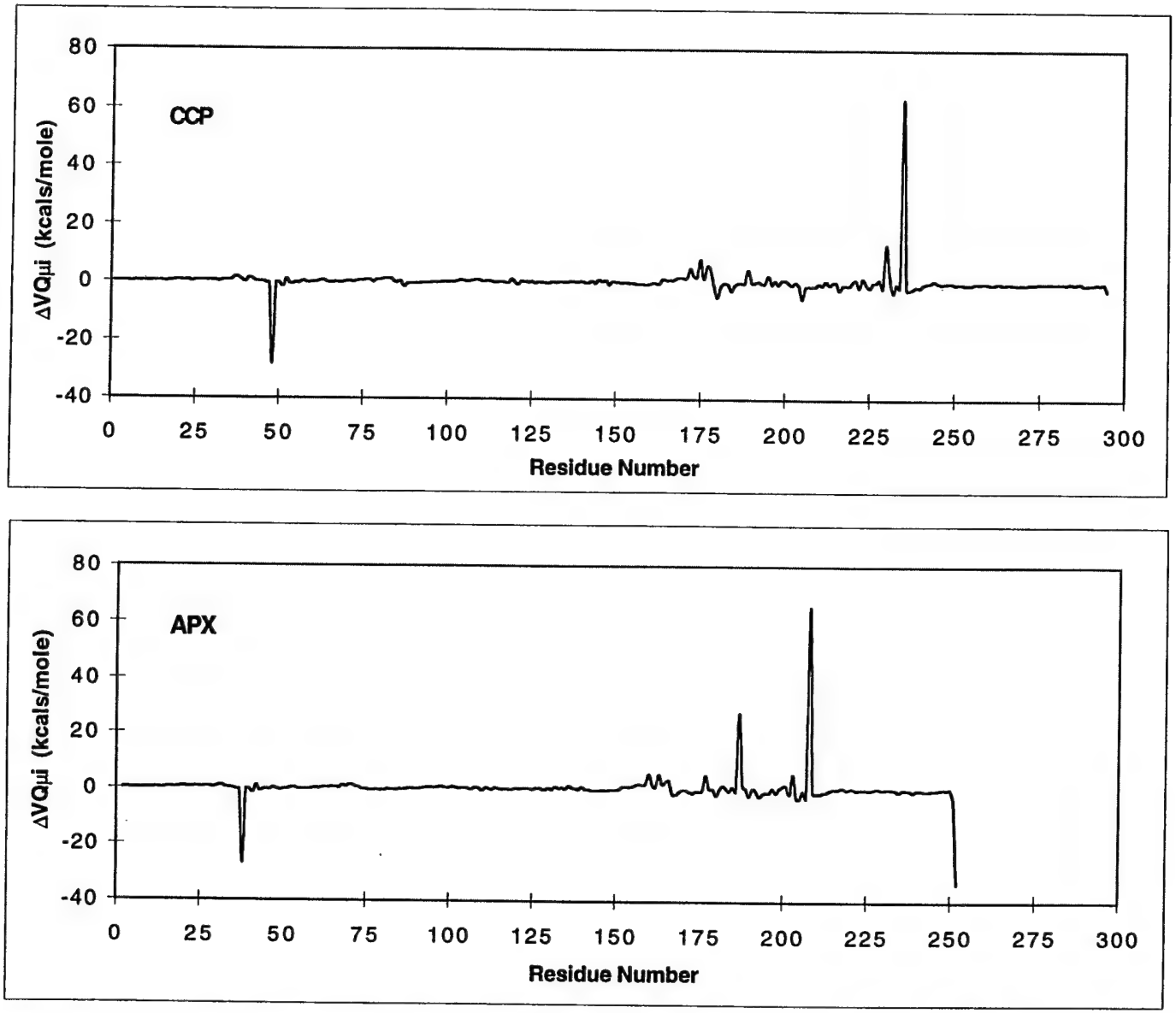

Figure 5. ΔVQμi (the Contribution to ΔVQμ for the Redox Transition From Each Amino Acid i). The Last Entries for CCP and APX (Monomer A) Are the Heme and the Heme and K+ Atom, Respectively. Note That for the Sign Convention Employed Here, a Positive Value of a ΔVQμi Is Electrostatically Stabilizing to a Cation Radical at the Triad Tryptophan.

Table 4. Contributions to ΔVQμ[a]

CCP Amino Acid	ΔVQμi (kcal/mol)	APX Amino Acid	ΔVQμi (kcal/mol)
Arginine 48 Guanadino	-28.3	Arginine 38 Guanadino	-26.9
Methionine 172 Carbonyl	5.0	Serine 160 Carbonyl	5.4
Histidine 175 Carbonyl	7.9	Histidine 163 Carbonyl	5.1
Leucine 177 Carbonyl	5.8	Isoleucine 165 Carbonyl	2.7
Threonine 180 [b]	-5.0	Alanine 168 Carbonyl	-1.7
Glycine 189 Carbonyl	4.0	Glycine 177 Carbonyl	5.0
Phenylalanine 202	-0.6	Tyrosine 190 Carbonyl	-2.4
Asparagine 205 Carbonyl	-5.4	Glutamate 193 Carbonyl	-2.4
Methionine 230 [b]	13.2	Leucine 203 Carbonyl	5.3
Methionine 231 [b]	1.4	Glutamate 204 [b]	-3.1
Leucine 232 Amide NH	-3.3	Leucine 205 Amide NH	-3.7
Aspartate 235 Carboxylate	63.2	Aspartate 208 Carboxylate	65.8
—	—	Aspartate 187 Carboxylate	27.5
—	—	Potassium Cation	-33.8
—	—	Aspartate 187/K+ Pair	-6.3

[a] For APX, the ΔVQμi values are averages of structures A through D (See Methods). Residues in CCP and APX are paired to represent structurally homologous amino acids. Where a Carbonyl contributes, the NH moiety of that Amide will also generally contribute. The converse is also generally true.

[b] For threonine 180 and methionine 230/231 in CCP, and for glutamine 204 in APX, both side chain and carbonyl contribute.

radical is reported to form in this mutant. So while methionine 230 provides stabilization to the tryptophan radical in CCP relative to leucine 203 in APX, mutation at this site results in relatively little change in overall electrostatic stabilization of a tryptophan radical. This illustrates the point that a given moiety (e.g., an amino acid side chin) can contribute to the electrostatic destabilization of a redox process, but upon mutation, the system (protein structure, polarity, and solvent) can "relax" to (partially) accommodate the change.

The most striking factor noted in the structure of APX relative to CCP was the presence of the potassium site. This cation site has been proposed [11, 12, 13, 55] as a possible mechanism for electrostatic destabilization of a tryptophan-179 radical in APX. Consistent with this proposal, the electrostatic contributions in Table 4 of the K+ and the ligand aspartate-187 are significant and find no analog in CCP. However, the ion-pair forms a dipole (see Table 4), which, while favorably oriented to destabilize a cation at tryptophan-179, is some 9-10Å away, with both intervening solvent and polypeptide medium in between (Figure 1) [11–13]. The PDLD model can evaluate this interaction without assumption of a bulk dielectric constant for this composite medium [56], and we have examined the effects of eliminating the charges on the aspartate-K+ pair in APX. Results for these calculations are reported in Table 2 for x-ray-derived structures and in Table 3 for MD-averaged calculations. For the x-ray-derived structures without MD averaging, the data in Table 2 show that the aspartate-K+ ion-pair contributes relatively little to destabilizing the tryptophan cation radical. Without the charged ion-pair, the average $\Delta\Delta V$ was −260 mV, only 19 mV smaller than the corresponding calculation with the aspartate-K+ dipole present. As before, a spread of values is observed for structures A–D, and MD averaging again reduces the spread between these structures. After including MD averaging (MD, structures A–D), we obtained $\Delta\Delta V$ between the ion-pair charge deleted structures and CCP of −7.1 kcal/mole, which corresponds to −308 mV, only ~20 mV different from $\Delta\Delta V$, which includes the ion pair. From this result, it can be concluded that the aspartate-K+ pair does play a role in destabilizing a cation radical at tryptophan-179 in APX but is only one of several factors. Of significant interest, a recent study reported the engineering of a K+ binding site in CCP by site-directed mutagenesis at the analogous position to that of APX [13] resulting in a significant destabilization of the tryptophan-191 radical [57–60].

Absolute errors in the calculations presented here are expected to be significant, but are reduced substantially by the problem posed (comparing electrostatic stabilization of a single species in two very similar environments). Modeling of the aspartate-tryptophan interaction is at this point purely electrostatic, without consideration of hydrogen bonding. The heme is treated as overall eletroneutral, but of course in CCP this group also undergoes oxidation from a formally cationic to a neutral state. Molecular dynamics required unsophisticated Cartesian constraints on the histidine heme ligand, triad aspartate-tryptophan, as well as on the aspartate-K+ pair. With the exception of the latter, all of these approximations are common to both structures and therefore are not expected to translate into significant errors in $\Delta\Delta V$. While the *ab initio* methods used to obtain ESP charges are quite sophisticated, they represent an *in vacuo* state of the 3-methylindole molecule. Examining the effect of the highly charged CCP environment (specifically, the charge on aspartate 235 and the amide groups from residues 175 and 177) on these charges revealed only very small changes in charge distribution (Table 1). Calculations of ΔV and $\Delta\Delta V$ were similarly affected very little by these different charges (data not shown). Although the solvent model employed in the determination of ΔVL is a microscopic model, it falls short of a full modeling of the aqueous environment. Figure 6 shows the number distribution and energy distributions of individual dipoles contributing to ΔVL. Clearly, modeling of solvent in a reasonably sophisticated manner will improve the accuracy of any calculation of $\Delta\Delta V$.

Calculations of the electrostatic environment of tryptophan-179 of APX relative to tryptophan-191 of CCP have been reported previously [11–13]. A continuum model was used with dielectric constants of either 2 or 9. Charge parameters for the tryptophan cation radical were not specified. These studies clearly demonstrated a more positive ESP in APX relative to CCP and also suggested a partial role for the K+ atom in establishing this difference in potential. However, quantitative interpretation of these results must suffer from the arbitrary choice of dielectric, which can vary enormously for different interactions, with or without significant presence of solvent water (see discussion in Jensen, Warshel, and Stephens [26] and Warshel, Papzyan, and Muegge [56]). Even relative comparisons (e.g., $\Delta\Delta V$ for APX vs. CCP) may be difficult to derive using continuum methods, since the specific between group effective dielectric constants [61] may be different for different interactions (e.g., triad aspartate-tryptophan vs. K+-tryptophan). The present calculations

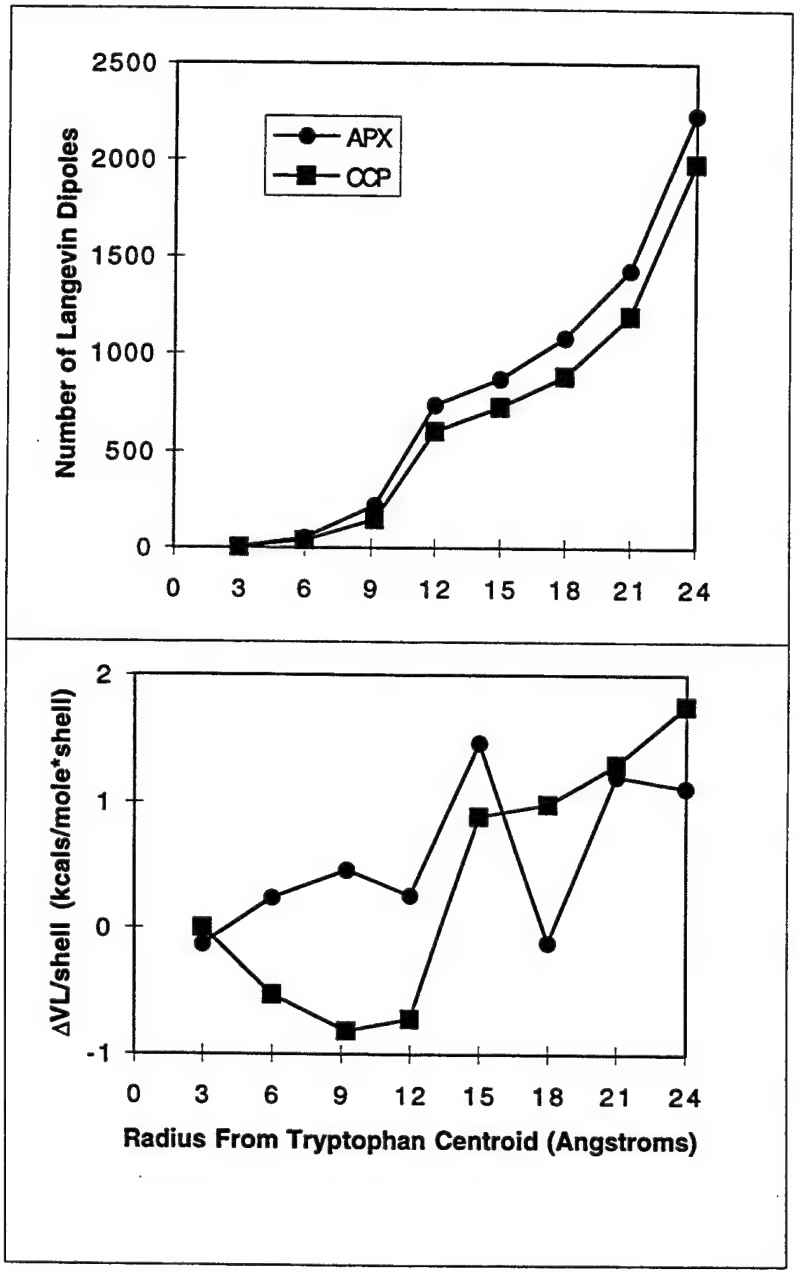

Figure 6. Upper Plot: Cumulative Occurrence of Langevin Dipoles Moving Radially Away From the Geometric Centroid of the Triad Tryptophan in CCP and APX (Structure A). Lower Plot: Energetic Contribution to ΔVL for CCP and APX of Each 3Å Shell (0–3Å, 3–6Å, etc.).

expand on the previous work in part by including realistic modeling of the tryptophan radical, protein polarization, MD structure averaging, and a microscopic solvent model, and provide quantitative estimates of the difference in redox potential for the active site tryptophan between CCP and APX, as well as the magnitude of the principle factors that contribute to this difference.

4. References

1. Rees, D. C., D. Farrelly, D. S. Sigman, and P. D. Boyer (Eds.). *The Enzymes*. NY: Academic Press, vol. 19, pp. 37–97.

2. Dawson, J. H. *Science*. Vol. 246, pp. 433–439, 1988.

3. Poulos, T. L. *Advanced Inorganic Biochemistry*. Vol. 7, pp. 1–33, 1988.

4. Sivaraja, M., D. B. Goodin, M. Smith, and B. M. Hoffman. *Science*. Vol. 245, pp. 738–740, 1989.

5. Erman, J. E., L. B. Vitello, J. M. Mauro, and J. Kraut. *Biochemistry*. Vol. 28, pp. 7992–7995, 1989.

6. Scholes, C. P., Y. Liu, L. A. Fishel, M. F. Farnum, J. M. Mauro, and J. Kraut. *Israel Journal of Chemistry*. Vol. 29, pp. 85–92, 1989.

7. Houseman, A. L. P., P. E. Doan, D. B. Goodin, and B. M. Hoffman. *Biochemistry*. Vol. 32, pp. 4430–4443, 1993.

8. Huyett, J. E., P. E. Doan, R. Gurbriel, A. L. P. Houseman, M. Sivaraja, D. B. Goodman, and B. M. Hoffman. *Journal of American Chemical Society*. Vol. 117, pp. 9033–9041, 1995.

9. Jensen, G. M., D. B. Goodin, and S. W. Bunte. *Journal of Physical Chemistry*. Vol. 100, pp. 954–959, 1996.*

10. Goodin, D. B., and D. E. McRee. *Biochemistry*. Vol. 32, pp. 3313–3324, 1993.

11. Patterson, W. R., and T. L. Poulos. *Biochemistry*. Vol. 34, pp. 4331–4341, 1995.

12. Pappa, H., W. R. Patterson, and T. L. Poulos. *Biological Inorganic Chemistry*. Vol. 1, pp. 61–66, 1996.

13. Bonagura, C. A., M. Sundaramoorthy, H. S. Pappa, W. R. Patterson, and T. L. Poulos. *Biochemistry*. Vol. 35, pp. 6107–6115, 1996.

14. Patterson, W. R., T. L. Poulos, and D. B. Goodin. *Biochemistry*. Vol. 34, pp. 4342–4345, 1995.

* This paper calculates, *inter alia*, spin densities for the cation radical of 3-methylindole. Like the cationic charge distribution reported here as partial atomic charges, the spin density of the cation radical is distributed over the whole of the indole moiety.

15. Finzel, B. C., T. L. Poulos, and J. Kraut. *Journal of Biological Chemistry.* Vol. 259, pp. 13027–13036, 1984.

16. Liu, R., M. A. Miller, G. W. Han, S. Hahm, L. Geren, S. Hibdon, J. Kraut, B. Durham, and F. Millett. *Biochemistry.* Vol. 33, pp. 8678–8685, 1994.

17. Warshel, A. *Computer Modeling of Chemical Reactions in Enzymes and Solutions.* NY: Wiley-Interscience, 1991.

18. Lee, F. S., Z. T. Chu, and A. Warshel. *Journal of Computational Chemistry.* Vol. 14, pp. 161–185, 1993.

19. Muegge, I., P. X. Qi, A. J. Wand, Z. T. Chu, and A. J. Warshal. *Journal of Physical Chemistry.* Vol. 101, pp. 825–836, 1997.

20. Sham, Y. Y., Z. T. Chu, and A. J. Warshel. *Journal of Physical Chemistry.* Vol. 101, pp. 4458–4472, 1997.

21. Churg, A., and A. Warshel. *Biochemistry.* Vol. 25, pp. 1675–1681, 1986.

22. Cutler, R. L., A. M. Davies, S. Creighton, A. Warshel, G. R. Moore, M. Smith, and A. G. Mauk. *Biochemistry.* Vol. 28, pp. 3188–3197, 1989.

23. Langen, R., G. D. Brayer, A. M. Berghuis, G. McLendon, F. Sherman, and A. J. Warshel. *Journal of Molecular Biology.* Vol. 224, pp. 589–600, 1992.

24. Parson, W. W., Z. T. Chu, and A. Warshel. *Biochemica Biophysica Acta.* Vol. 1017, pp. 251–272, 1990.

25. Langen, R., G. M. Jensen, U. Jacob, P. J. Stephens, and A. J. Warshel. *Biological Chemistry.* Vol. 267, pp. 25625–25627, 1992.

26. Jensen, G. M., A. Warshel, P. J. Stephens. *Biochemistry.* Vol. 33, pp. 10911–10924, 1994.

27. Jensen, G. M., Ph.D. *Dissertation*, University of Southern California, 1994.

28. Stephens, P. J., D. R. Jollie, and A. Warshel. *Chemical Reviews.* Vol. 96, pp. 2491–2513, 1996.

29. Bunte, S. W., G. M. Jensen, K. L. McNesby, D. B. Goodin, C. F. Chabalowski, S. Suhai, and K. J. Jalkanen. *Journal of Physical Chemistry* (submitted).

30. Stephens, P. J., F. J. Devlin, C. F. Chabalowski, and M. J. Frisch. *Journal of Physical Chemistry.* Vol. 98, pp. 11623–11627, 1994.

31. Stephens, P. J., F. J. Devlin, C. S. Ashvar, C. F. Chabalowski, and M. J. Frisch. *Faraday Discussion.* Vol. 99, pp. 103–119, 1994.

32. Frisch, M. W., *et al.* Gaussian, Inc., Pittsburgh, PA, 1995. Gaussian 92/DFT; Gaussian 94 (Revision B.1).

33. Hehre, W. J., L. Radom, P. R. Schleyer, and J. A. Pople. *Ab Initio Molecular Orbital Theory.* NY: Wiley, 1996.

34. Adamo, C., V. Barone, and A. Fortunelli. *J. Chem. Phys.* Vol. 102, pp. 384–393, 1995.

35. Qin, Y., and R. A. Wheeler. *J. Chem. Phys.* Vol. 102, pp. 1689–1698, 1995.

36. Singh, U. C., and P. A. Kollman. *Journal of Computational Chemistry.* Vol. 5, pp. 145–159, 1984.

37. Besler, B. H., K. M. Merz Jr., and P. A. Kollman. *Journal of Computational Chemistry.* Vol. 11, pp. 431–439, 1990.

38. McRee, D. E. *Journal of Molecular Graphics.* Vol. 10, pp. 44–46, 1992.

39. Hall, G. G., and C. M. Smith. *Int. J. Quant. Chem.* Vol. 25, pp. 881–890, 1984.

40. Smith, C. M., and G. G. Hall. *Theo Chimica Acta.* Vol. 69, pp. 63–69, 1986.

41. Mittler, R., and B. Zilinskas. *Federation of European Biochemical Societies Letters.* Vol. 289, pp. 257–259, 1991.

42. Mondal, M. S., H. A. Fuller, and F. A. Armstrong. *Journal of American Chemical Society.* Vol. 118, pp. 263–264, 1996. See also Mondal, M. S., D. B Grodin, and F. A. Armstrong. *Journal of American Chemical Society.* Vol. 120, pp. 6270–6276, 1998.

43. Jovanovic, S. V., S. Steenken, and M. G. Simic. *Journal of Physical Chemistry.* Vol. 95, pp. 684–687, 1991.

44. Fitzgerald M. M., M. J. Churchill, D. E. McRee, and D. B. Goodin. *Biochemistry.* Vol. 33, pp. 3807–3818, 1994.

45. Miller, M. A., G. W. Han, and J. Kraut. *Proceedings of the National Academy of Science.* U.S.A., vol. 19, pp. 11118–11122, 1994.

46. McRee, D. E., G. M. Jensen, M. M. Fitzgerald, H. A. Siegel, and D. B. Goodin. *Proceedings of the National Academy of Science.* U.S.A., vol. 91, pp. 12847–12851, 1994.

47. Fitzgerald, M. M., M. L. Trester, G. M. Jensen, D. E. McRee, and D. B. Goodin. *Protein Science*. Vol. 4, pp. 1844–1850, 1995.

48. Goodin, D. B. *Journal of Biological Inorganic Chemistry*. Vol. 1, pp. 360–363, 1996.

49. Fitzgerald, M. M., R. A. Musah, D. E. McRee, and D. B. Goodin. *Nature Structural Biology*. Vol. 3, pp. 626–631, 1996.

50. Sun, J., M. M. Fitzgerald, D. B. Goodin, and T. M. Loehr. *Journal of American Chemical Society*. Vol. 119, pp. 2064–2065, 1997.*

51. Musah, R. A., and D. B. Goodin. *Biochemistry*. Vol. 36, pp. 11665–11674, 1997.

52. Musah, R. A., G. M. Jensen, R. J. Rosenfeld, D. E. McRee, D. B. Goodin, and S. W. Bunte. *Journal of American Chemical Society*. Vol. 119, pp. 9083–9084, 1997.

53. Cao, Y., R. A. Musah, S. K. Wilcox, D. B. Goodin, and D. E. McRee. *Protein Science*. Vol. 7, pp. 72–78, 1998.

54. Fülöp, V., R. P. Phizackerley, S. M. Soltis, I. J. Clifton, S. Wakatsuki, J. Erman, J. Hajdu, and S. L. Edwards. *Structure*. Vol. 2, pp. 201–208, 1994.

55. Poulos, T. L., W. R. Patterson, and M. Sandaramoorthy. *Biochemical Society Transactions*. Vol. 23, pp. 228–232, 1995.

56. Warshel, A., A. Papzyan, and I. Muegge. *Journal of Biological Inorganic Chemistry*. Vol. 2, pp. 143–152, 1997.

57. Mauro, J. M., L. A. Fishel, J. T. Hazzard, T. E. Meyer, G. Tollin, M. A. Cusanovich, and J. Kraut. *Biochemistry*. Vol. 27, pp. 6243–6256, 1988.*

58. Roe, J. A., and D. B. Goodin. *Journal of Biological Chemistry*. Vol. 268, pp. 20037–20045, 1993.*

59. Choudhury, K., M. Sundaramoorthy, A. Hickman, T. Yonetani, E. Woehl, M. F. Dunn, and T. L. Poulos. *Journal of Biological Chemistry*. Vol. 269, pp. 20239–20249, 1994.*

60. Wilcox, S. K., G. M. Jensen, M. M. Fitzgerald, D. E. McRee, and D. B. Goodin. *Biochemistry*. Vol. 35, pp. 4858–4866, 1996.*

61. Rees, D. C. *J. Mol. Biol.* Vol. 141, pp. 323–326, 1980.

---

* For mutagenesis studies aimed at redirecting the substrate specificity of CCP, also see McRee et al. [46], Musah and Goodin [51], Mauro et al. [57], Roe and Goodin [58], Choudhury et al. [59], and Wilcox et al. [60].

NO. OF COPIES ORGANIZATION

2 DEFENSE TECHNICAL INFORMATION CENTER
DTIC DDA
8725 JOHN J KINGMAN RD
STE 0944
FT BELVOIR VA 22060-6218

1 HQDA
DAMO FDQ
D SCHMIDT
400 ARMY PENTAGON
WASHINGTON DC 20310-0460

1 OSD
OUSD(A&T)/ODDDR&E(R)
R J TREW
THE PENTAGON
WASHINGTON DC 20301-7100

1 DPTY CG FOR RDE HQ
US ARMY MATERIEL CMD
AMCRD
MG CALDWELL
5001 EISENHOWER AVE
ALEXANDRIA VA 22333-0001

1 INST FOR ADVNCD TCHNLGY
THE UNIV OF TEXAS AT AUSTIN
PO BOX 202797
AUSTIN TX 78720-2797

1 DARPA
B KASPAR
3701 N FAIRFAX DR
ARLINGTON VA 22203-1714

1 NAVAL SURFACE WARFARE CTR
CODE B07 J PENNELLA
17320 DAHLGREN RD
BLDG 1470 RM 1101
DAHLGREN VA 22448-5100

1 US MILITARY ACADEMY
MATH SCI CTR OF EXCELLENCE
DEPT OF MATHEMATICAL SCI
MAJ M D PHILLIPS
THAYER HALL
WEST POINT NY 10996-1786

NO. OF COPIES ORGANIZATION

1 DIRECTOR
US ARMY RESEARCH LAB
AMSRL D
J W LYONS
2800 POWDER MILL RD
ADELPHI MD 20783-1145

1 DIRECTOR
US ARMY RESEARCH LAB
AMSRL DD
J J ROCCHIO
2800 POWDER MILL RD
ADELPHI MD 20783-1145

1 DIRECTOR
US ARMY RESEARCH LAB
AMSRL CS AS (RECORDS MGMT)
2800 POWDER MILL RD
ADELPHI MD 20783-1145

3 DIRECTOR
US ARMY RESEARCH LAB
AMSRL CI LL
2800 POWDER MILL RD
ADELPHI MD 20783-1145

ABERDEEN PROVING GROUND

4 DIR USARL
AMSRL CI LP (305)

NO. OF
COPIES ORGANIZATION

1 NEXSTAR PHARMACEUTICALS INC
G M JENSEN
650 CLIFFSIDE DRIVE
SAN DIMAS CA 91773

2 THE SCRIPPS RSRCH INSTITUTE
DEPT OF MOLECULAR BIOLOGY
D B GOODIN
MB8
10550 N TORREY PINES RD
LA JOLLA CA 92037

REPORT DOCUMENTATION PAGE

Form Approved
OMB No. 0704-0188

1. AGENCY USE ONLY *(Leave blank)*	2. REPORT DATE	3. REPORT TYPE AND DATES COVERED
	December 1998	Final, Aug 96 - Oct 97

4. TITLE AND SUBTITLE
Energetics of Cation Radical Formation at the Proximal Active Site Tryptophan of Cytochrome-*c*- Peroxidase and Ascorbate Peroxidase

5. FUNDING NUMBERS
1L161102AH43

6. AUTHOR(S)
G. M. Jensen, S. W. Bunte, A. Warshel, and D. B. Goodin

7. PERFORMING ORGANIZATION NAME(S) AND ADDRESS(ES)
U.S. Army Research Laboratory
ATTN: AMSRL-WM-BD
Aberdeen Proving Ground, MD 21005-5066

8. PERFORMING ORGANIZATION REPORT NUMBER
ARL-TR-1859

9. SPONSORING/MONITORING AGENCY NAMES(S) AND ADDRESS(ES)

10.SPONSORING/MONITORING AGENCY REPORT NUMBER

11. SUPPLEMENTARY NOTES
* G. M. Jensen and D. B. Goodin are with the Department of Molecular Biology, The Scripps Research Institute.
† A. Warshel is with the Department of Chemistry, University of Southern California.

12a. DISTRIBUTION/AVAILABILITY STATEMENT
Approved for public release; distribution is unlimited.

12b. DISTRIBUTION CODE

13. ABSTRACT *(Maximum 200 words)*

Despite very similar protein structures, ascorbate peroxidase (APX) and yeast cytochrome-*c*-peroxidase (CCP) stabilize different radical species during enzyme turnover. Both enzymes contain similar active site residues, including the tryptophan that is oxidized to a stable cation radical in CCP. However, the analogous trytophan is not oxidized in APX, and the second oxidizing equivalent is retained as a porphyrin π-cation radical. In this study, we provide an improved computational approach to estimate the contribution of solvent and protein electrostatics to the energetics of tryptophan cation radical formation in the two enzyme environments. The Protein Dipoles Langevin Dipoles (PDLD) model is combined with molecular dynamics to estimate the role of discrete solvation, atomic polarizabilities, and dynamic motional averaging on the electrostatic potentials. The PDLD model shows that the protein environment of CCP stabilizes the tryptophan cation radical by 330 mV relative to that in APX. Analysis of the components contributing to this difference supports proposals that the cation binding site contributes to, but is not the sole cause of, the different sites of radical stabilization. The enzymes have thus evolved this distinction using several contributing interactions including the cation binding site, solvent access, and subtle differences in protein structure and dynamics.

14. SUBJECT TERMS
tryptophan, oxidation, electrostic modeling

15. NUMBER OF PAGES
35

16. PRICE CODE

17. SECURITY CLASSIFICATION OF REPORT	18. SECURITY CLASSIFICATION OF THIS PAGE	19. SECURITY CLASSIFICATION OF ABSTRACT	20. LIMITATION OF ABSTRACT
UNCLASSIFIED	UNCLASSIFIED	UNCLASSIFIED	UL

INTENTIONALLY LEFT BLANK.

USER EVALUATION SHEET/CHANGE OF ADDRESS

This Laboratory undertakes a continuing effort to improve the quality of the reports it publishes. Your comments/answers to the items/questions below will aid us in our efforts.

1. ARL Report Number/Author ARL-TR-1859 (Jensen) Date of Report December 1998\

2. Date Report Received _____

3. Does this report satisfy a need? (Comment on purpose, related project, or other area of interest for which the report will be used.) _____

4. Specifically, how is the report being used? (Information source, design data, procedure, source of ideas, etc.) _____

5. Has the information in this report led to any quantitative savings as far as man-hours or dollars saved, operating costs avoided, or efficiencies achieved, etc? If so, please elaborate. _____

6. General Comments. What do you think should be changed to improve future reports? (Indicate changes to organization, technical content, format, etc.) _____

CURRENT ADDRESS

Organization

Name E-mail Name

Street or P.O. Box No.

City, State, Zip Code

7. If indicating a Change of Address or Address Correction, please provide the Current or Correct address above and the Old or Incorrect address below.

OLD ADDRESS

Organization

Name

Street or P.O. Box No.

City, State, Zip Code

(Remove this sheet, fold as indicated, tape closed, and mail.)

(DO NOT STAPLE)